GEOPHYSICAL RESEARCH LETTERS, VOL. 28, NO. 13, PAGES 2541-2544, JULY 1, 2001

Seismological *in situ* Estimation of Density Jumps across the Transition Zone Discontinuities beneath Japan

Mamoru Kato [1] and Hitoshi Kawakatsu

Earthquake Research Institute, University of Tokyo, Tokyo, Japan

Abstract. We investigate the magnitude of shear-wave velocity and density jumps across the 410-km and 660-km discontinuities in the Earth's mantle. We estimate SS reflection and PS conversion coefficients from *ScS* reverberations and receiver-side P-S converted phases, respectively, using broadband seismograms recorded at stations in western Japan. Fractional changes of model parameters that satisfy our observations in the northwest Pacific are (ΔVs, $\Delta\rho$)= (8.5%, 5.4%) for the 660-km discontinuity, and (4.9%, 1.9%) for the 410-km discontinuity.

Introduction

Density jumps across the transition zone discontinuities partly control the style of convection in the Earth's mantle. For a better understanding of the evolution of this planet, we ought to know how large these jumps are at the 410-km and 660-km discontinuities. The transition zone discontinuities are often associated with major phase transitions of olivine minerals, but recent models predict that garnet minerals also play major roles at the upper-lower mantle boundary [*Vacher et al*, 1998]. We can measure densities of constituent mantle minerals at high pressure and temperature in the laboratory, and seismological observations of *in situ* density would be assets in modeling mineralogy in the transition zone.

Seismologically speaking, *in situ* density is not easy to estimate directly. Resolution of low frequency seismology [e.g., *Tanimoto,* 1991] is not sufficient to resolve the sharp transition zone discontinuities. One indirect but practical approach is to estimate seismic reflection and transmission coefficients at mantle discontinuities. Densities and velocities at both sides of discontinuities determine these coefficients, but their dependence is complicated, and previous studies often rely on external scaling laws.

Each reflection or transmission coefficient has different dependence on velocities and density, but uncertainties in models can be substantially reduced by combining more than one measurement. We estimate the magnitude of density jumps at the transition discontinuities from two observations of the coefficients, namely SS near-vertical reflection and PS conversion coefficients; the former is determined by both shear-wave velocity and density jumps, while the latter is strongly controlled by the shear-wave velocity jump. We employ broadband seismograms recorded at high density regional arrays in Japan, J-Array and FREESIA, to estimate these coefficients. The target area is the Pacific side of western Japan (Fig. 1), where tomographic studies have implicated slab stagnation in the transition zone [e.g., *Fukao et al.,* 2001].

SS reflection coefficients

SS reflection coefficients (SH-to-SH reflection coefficients, to be precise) are estimated from *ScS* reverberation waveforms [*Kato et al.*, 2001]. *ScS* reverberation phases sample mantle discontinuities with redundancy, and are suited to estimate path-averaged properties [*Revenaugh and Jordan*, 1991]. Ray paths of *ScS* reverberations are nearly vertical in regional distances, and we can estimate SS reflection coefficients for normal incidence.

We use broadband waveforms of a deep event in Izu (Aug. 20, 1998) recorded at stations in western Japan (Fig. 1a). Band-pass filtered (5-30 mHz), transverse component seismograms from 11 broadband stations are stacked together to form a data seismogram (Fig. 2). We estimate path-averaged properties of the mantle as well as of major discontinuities via a multi-step grid search optimization. Goodness of models is evaluated with cross-correlation coefficients between ray-theoretical synthetic seismograms and the data seismogram (Fig. 2). Uncertainty bounds of the model parameters are estimated from the distribution of resultant cross-correlation coefficients, assuming χ^2 statistics. Details are presented in *Kato et al.* [2001].

Estimated SS reflection coefficients in this region (Region A of *Kato et al.* [2001]) are 3.4 $\pm$ 0.3% and 6.9 $\pm$ 0.3% for the 410-km and 660-km discontinuities, respectively (Fig. 3). These values are consistent with the earlier results by *Revenaugh and Jordan* [1991] in this region (corridor 10), 3.7 $\pm$ 1.0 % and 6.6 $\pm$ 1.0 %, respectively.

PS conversion coefficients

P-to-S converted phases from the receiver-side discontinuities have been extensively used to map topography of the discontinuities [e.g., *Niu and Kawakatsu*, 1996]. *P410s* and *P660s* phases, conversion at the 410-km and 660-km discontinuities, arrive approximately 42 and 68 seconds after the direct *P*, respectively, at 71.4°, which is the average epicentral distance for our dataset.

We process 76 sets of broadband seismograms from 9 events in the Fiji region that were recorded at stations in western Japan (Fig. 1b). Original three-component seismograms are rotated into P-SV-SH coordinate [*Vinnik*, 1977] after filtered in the 50-200 mHz band. We estimate an empirical source time function for each event from direct *P* on P component seismograms at stations in western as well as eastern Japan. This is deconvolved from traces of the cor-

[1]Now at School of Earth Sciences, Faculty of Integrated Human Studies, Kyoto University, Kyoto, Japan.

Paper number 2000GL012747.
0094-8276/01/2000GL012747$05.00

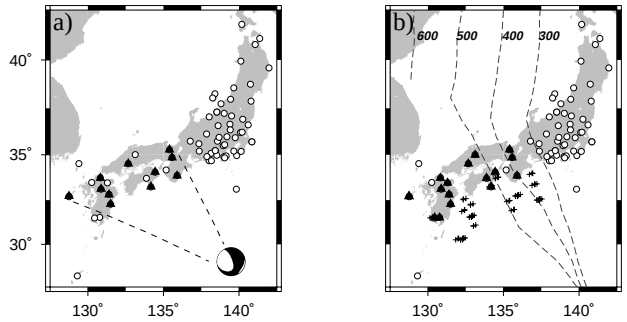

Figure 1. Map of study area. a) For *ScS* reverberation study [*Kato et al.*, 2001]. Triangles are stations we used. Harvard CMT solution is plotted at the epicentral location. b) For P-S conversion study. Triangles indicate stations we use. Pluses show the ray-theoretical conversion points for *P660s* phases. Dash lines show the contour of deep seismicity. Open circles in both panels indicate unused stations.

responding event to equalize the source spectra. Resultant traces are normalized by the amplitude of corresponding direct P, and SV component traces are stacked in slowness-time domain to enhance converted phases. Proximity of the stations, however, limits resolution of slowness. AK135 [*Kennett et al.*, 1995] is our reference model for ray theoretical parameters.

We derive PS conversion coefficients from amplitude ratios of P and the later phases (Fig. 2), and employ the jackknife method to estimate their uncertainty bounds. Differential attenuation in the receiver-side upper mantle is corrected using our estimate of Q_{ScS} in this region, 165 [*Kato et al.*, 2001], assuming $Q_P/Q_S = 9/4$. PP transmission coefficients are not unity for the current ray geometry, which are corrected using AK135. We assume that topography of discontinuities are negligible. When the discontinuities have large topography, arrival times and amplitudes of converted phases should have large scatters. This appears not to be the case for our results, since estimation errors of the stacked traces (Fig. 2) are not particularly large in the vicinity of expected arrivals of these phases.

Our estimates of PS coefficients at the 410-km and 660-km discontinuities are 2.7 ± 0.8 %, and 6.0 ± 0.7 %, respectively (Fig. 3). Relatively large uncertainty for the 410-km discontinuity is due to the smaller amplitude and lesser signal-to-noise ratio of the *P410s* phase.

Results

Our model parameters are fractional changes of density ($\Delta\rho$), and shear-wave velocity (ΔVs), which are ratios of the difference to the average of densities, and shear-wave velocities, across the discontinuities, respectively. We assume isotropy for the media. We assume AK135 values for compressional-wave velocities; PS conversion coefficients have negligible sensitivity on their perturbation when reasonable mantle velocities are assumed as reference models. The model that simultaneously satisfies both observations is our best model for each discontinuity. We delineate associated confidence ellipsoids using uncertainty bounds of both coefficients assuming χ^2 statistics.

Our best models are (ΔVs, $\Delta\rho$) = (4.9%, 1.9%), and (8.5%, 5.4%) for the 410-km and 660-km discontinuities, respectively (Fig. 3). Uncertainty bounds for 1σ are approximately 1.5 and 1% for the respective discontinuities.

Our estimates of reflection and conversion coefficients are in different frequency bands owing to the different signal spectra of the target phases; characteristic periods are approximately 40 and 15 seconds for *ScS* reverberations and *Pds* phases, respectively. We assume that the discontinuities are of first-order, and that reflection and transmission coefficients are frequency independent. This could be

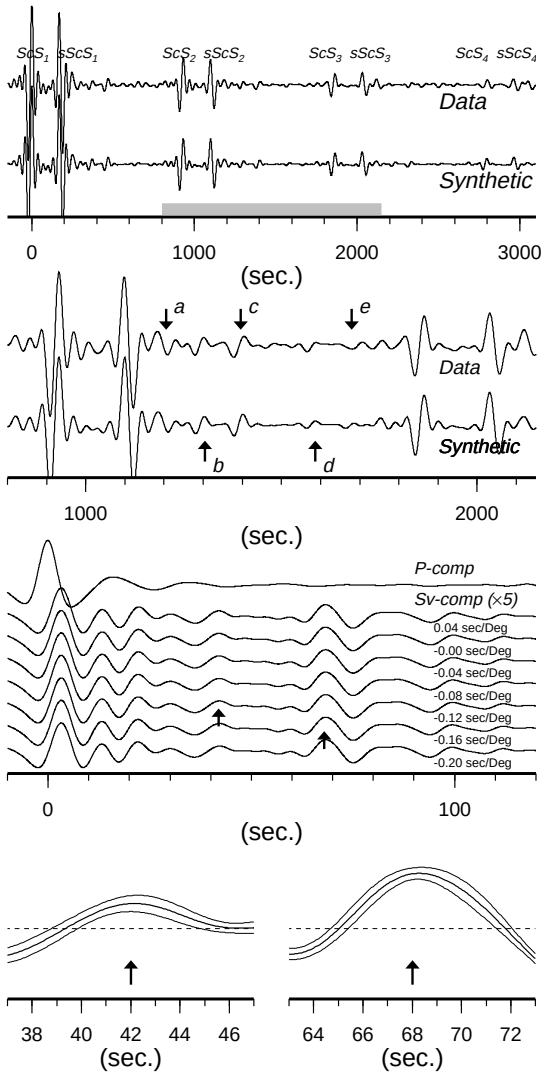

Figure 2. (top panel) Stacked, and synthetic seismograms calculated for the best fitting model in ScS reverberation study. Origin of time axis is at ScS phase. Four pairs of large amplitude phases are $\{ScS_n, sScS_n\}$ (n=1–4). (second panel) Close up of the waveforms between ScS_2 and $sScS_3$ (marked by a gray line in the top panel). Notable 1st order phases are labeled; a) $\{ScS_2, S660_+S\}$, b) $\{ScS_2, sS410_+S\}$, c) $\{ScS_2, sS660_+S\}$, d) $\{ScS_3, S660_-S\}$, and e) $\{ScS_3, S410_-S\}$. (third panel) Resultant stacked traces in *Pds* study. Shown are P-component, and SV-components stacked for various differential slownesses. *P410s* and *P660s* are marked by arrows at traces for corresponding slownesses. (bottom panels) Close up of *P410s* (left) and *P660s* phases (right). Dash lines are the zero lines. Accompanying thin lines indicate estimated $\pm 1\sigma$ uncertainties of stacked traces.

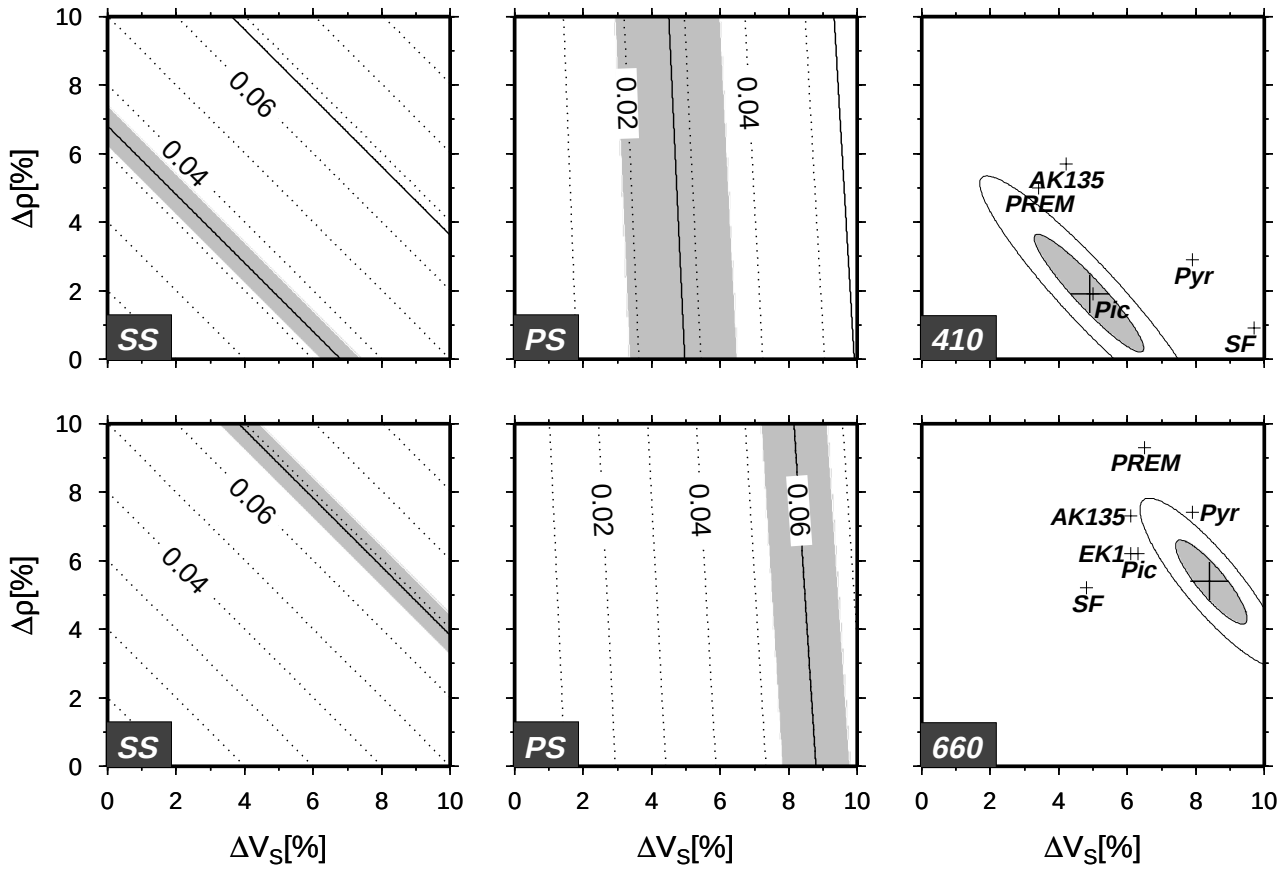

Figure 3. (From left to right, SS reflection coefficients, PS conversion coefficients, and results for the 410-km (top row) and the 660-km (bottom row) discontinuities. The best fitting model is shown by large crosses in the right columns, and 1σ and 2σ limits by shades and contour lines, respectively. Other data points are *AK135*: AK135 model, *PREM*: PREM model, *SF*: *Shearer and Flanagan* [1999], *EK1*: *Estabrook and Kind* [1996], and *Pic* and *Pyr*: piclogite and pyrolite models, respectively, of *Gaherty et al.* [1999] for the 410-km discontinuity, and of *Vacher et al.* [1998] for the 660-km discontinuity (cumulative jumps for 1500 K adiabat).

an over-simplification since mineralogy predicts otherwise, which some seismological observations have apparently supported (see *Helffrich* [2000] for a review). We would underestimate ΔVs and $\Delta\rho$ in cases that the discontinuities are of finite width and that velocities and densities gradually increase, such as the models in *Gaherty et al.* [1999].

The actual aspherical velocity structure in the mantle causes small shifts of relative travel times between the reference and target phases, which would result in reduction of stacked amplitude of the target phase. Our use of high density broadband arrays should minimize effects of incoherent stacking [*Revenaugh and Jordan*, 1991; *Flanagan and Shearer*, 1998], and we do not apply correction to the amplitude measurements. For the reference, *Revenaugh and Jordan* [1991] estimated that observed reflectivities are reduced as much as 10-20% by these two effects combined.

Discussion

Our best model for the 660-km discontinuity is more than 2σ away from AK135 and PREM. Small inconsistency with the global one-dimensional models is expected, since these models are parameterized with low-order polynomials and changes of velocity gradients near the discontinuities [e.g., *Vacher et al.*, 1998] are not properly represented. The large density jump at the 670-km discontinuity in PREM, nevertheless, appears to be incompatible with our observation, which is in accord with previous seismological studies [*Estabrook and Kind*, 1996; *Shearer and Flanagan*, 1999].

Our result for the 660-km discontinuity is more or less consistent with mineralogical predictions both for pyrolite and piclogite compositions (Fig. 3). A cold thermal anomaly due to the stagnant slab in this region is estimated to be at most 150 °C, and be localized at 660 km depth [*Kato et al.*, 2001]. $\Delta\rho$ and ΔVs are expected to increase slightly from normal values in such condition, but an extremely cold thermal anomaly (such as 1000 K adiabat cases by *Vacher et al.* [1998]) appears to be unlikely. For the 410-km discontinuity, a piclogitic composition [*Gaherty et al.*, 1999] would explain our observation adequately. Uncertainty of the model is still large, however, and this does not necessarily discriminate pyrolite from piclogite for the mantle composition.

Our estimates disagree with the global average by *Shearer and Flanagan* [1999], estimated from *PP* and *SS* precursors. We should expect lateral variation in the transition zone, and since the stagnant slab is tomographically imaged in our target region [e.g., *Fukao et al.,* 2001], our regional estimates are not necessarily required to agree with the global average. We should note, nevertheless, that our model satisfies the average SS reflection coefficients obtained by a different *ScS*

reverberation methodology for several regions, (4.2 ± 1.0 % and 5.9 ± 1.0 % for the 410-km and 660-km discontinuities, respectively) [*Revenaugh and Jordan*, 1991; *Revenaugh and Sipkin*, 1994], while the model of *Shearer and Flanagan* [1999] marginally do so; the 410-km discontinuity of their model has apparently a larger impedance contrast than the 660-km discontinuity. The agreement between our results and those by Revenaugh and co-workers would suggest that the postulated stagnant slab has minor effects on the $\Delta\rho$ and ΔVs at the transition zone discontinuities.

Uncertainties with models by ourselves and by *Shearer and Flanagan* [1999] are still large, sources of which include scatter in raw data, uncertainties in adopted assumptions (e.g., topography of the discontinuities, velocities and attenuation), complex propagation of *SS* and *PP* precursors [e.g., *Neele et al.* 1997], and probable heterogeneous structure of the discontinuities. Better understanding of our seismological tools and data is required to achieve a unified seismological model of the transition zone discontinuities.

Acknowledgments. J-Array and FREESIA data centers facilitated us for the access to the data archive. We appreciate comments by Y. Fukao, and T. Iidaka. Figures are created with GMT [*Wessel and Smith*, 1995].

References

Estabrook, C.H., R. Kind, The nature of the 660-kilometer upper-mantle seismic discontinuity from precursors to PP, *Science, 274,* 1179-1182, 1996.

Flanagan, M.P., and P.M. Shearer, Global mapping of topography on transition zone velocity discontinuities by stacking SS precursors, *J. Geophys. Res., 103,* 2673-2692, 1998.

Fukao, Y., S. Widiyantoro, and M. Obayashi, Stagnant slabs in the upper and lower mantle transition region, *Rev. Geophys.,* in press, 2001.

Gaherty, J.B., Y. Wang, T.H. Jordan, and D.J. Weidner, Testing plausible upper-mantle compositions using fine-scale models of the 410-km discontinuity, *Geophys. Res. Lett., 26,* 1641-1644, 1999.

Helffrich, G., Topography of the transition zone seismic discontinuities, *Rev. Geophys., 38,* 141-158, 2000.

Kato, M., M. Misawa, and H. Kawakatsu, Small subsidence of the 660-km discontinuity beneath Japan probed by ScS reverberations, *Geophys. Res. Lett., 28*, 447-450, 2001.

Kennett, B.L.N., E.R. Engdahl, and R. Buland, Constraints on seismic velocities in the Earth from traveltimes, *Geophys. J. Int., 122,* 108-124, 1995.

Neele, F., H. de Regt, and J. VanDecar, Gross errors in upper mantle discontinuity topography from PdP and SdS data, *Geophys. J. Int., 129,* 194-204, 1997.

Niu, F., and H. Kawakatsu, Complex structure of mantle discontinuities at the tip of the subducting slab beneath Northeast China; a preliminary investigation of broadband receiver functions, *J. Phys. Earth, 44,* 701-711, 1996.

Revenaugh, J., and T.H. Jordan, Mantle layering from ScS reverberations, 2. The transition zone, *J. Geophys. Res., 96,* 19,763-19,780, 1991.

Revenaugh, J., and S.A. Sipkin, Mantle discontinuity structure beneath China, *J. Geophys. Res., 99,* 21,911-21,927, 1994.

Shearer, P.M., and M.P. Flanagan, Seismic velocity and density jumps across the 410- and 660- kilometer discontinuities, *Science, 285,* 1545-1548, 1999.

Tanimoto, T., Waveform inversion for three-dimensional density and S wave structure, *J. Geophys. Res., 96,* 8167-8189, 1991.

Vacher, P., A. Mocquet, and C. Sotin, Computation of seismic discontinuity profiles from mineral physics: The importance of the non-olivine components for explaining the 660 km depth discontinuity, *Phys. Earth Planet. Inter., 106,* 275-298, 1998.

Vinnik, L.P., Detection of waves converted from P to S in the mantle, *Phys. Earth Planet. Inter., 15,* 39-45, 1977.

Wessel, P., and W.H.F. Smith, New version of the Generic Mapping Tools released, *Eos Trans. AGU, 76,* 329, 1995.

M. Kato, and H. Kawakatsu, Earthquake Research Institute, University of Tokyo, Bunkyo, Tokyo, 113-0032, Japan. (e-mail: mkato@eri.u-tokyo.ac.jp)

(Received December 11, 2000; revised March 12, 2001; accepted March 15, 2001.)